XLIII CILAMCE
21–25, November, 2022
FOZ DO IGUAÇU – PR – BRAZIL

Dynamic analysis of Baja-type vehicle subjected to excitation by irregular road profile

Laura D. V. Braz[1], Gabriel R. P. Reis[1], Guilherme Magnabosco[1], Letícia F. F. Miguel[1]

[1]*Programa de Pós-Graduação em Engenharia Mecânica (PROMEC), Federal University of Rio Grande do Sul*
Rua Sarmento Leite, 425, 90040-001, Porto Alegre, RS, Brazil
laura.dacoreggio@gmail.com, reisgabrielramires@gmail.com, guilhermemagnabosco1@gmail.com, letffm@ufrgs.br

Abstract. Automotive vehicles are complex dynamic systems that travel over uneven roads of different qualities. This interaction induces vibrations whose characteristics depend on the suspension system, speed, and pavement type, among other factors. Extended exposure to vibrations can be annoying and harmful to human health, depending on the acceleration levels. At Baja SAE competitions, small off-road vehicles are designed and built to withstand rough terrains. Therefore, knowing the vehicle's response to irregularities is relevant to ensuring compliance with safety requirements. In this paper, a computational routine is designed to evaluate the dynamic response of a BAJA-type vehicle to excitations induced by an irregular surface. A three-dimensional full-car model with eight degrees of freedom simulates the vehicle's vertical dynamics. The road surface roughness is modeled in the frequency domain using Power Spectral Density functions, which are converted to time-domain signals. The numerical integration of the equations of motion is made through Newmark's method. The code is validated using commercial software and data from the literature. The outputs are the displacement, velocity, and acceleration signals for each vehicle's degree of freedom. Results evidenced the suspension system's effect on damping vibration levels experienced by the driver in relation to the base motion of the wheels.

Keywords: Vehicle dynamics, Newmark's method, Road roughness.

1 Introduction

Automotive vehicles are complex dynamic systems that travel over rough roads, absorbing excitation forces. This excitation induces vibrations whose magnitude may vary according to the suspension parameters and geometric characteristics of the vehicle [1]. Extended exposure to greater acceleration levels than those established by ISO 2631:1997 [2] can be annoying and even harmful to the driver's health. Hence, knowing how the system will respond is critical to ensure that safety requirements are fullfilled.

For this, it is necessary to carry on a dynamic analysis that uses suspension and geometry parameters as input data, along with the profile of vertical displacements of the pavement surface. It allows one to obtain the system's response, evaluate the suspension system's performance, and verify vibration levels reaching the driver.

During Baja-SAE competitions, small off-road vehicles are designed and built to withstand rough terrains for long periods without damage, especially in the endurance race. This research aims to develop computational numerical codes to estimate the acceleration levels to which pilots and evaluators are subject when using a Baja-type vehicle during the competition promoted by SAE BRASIL [3], which defines the criteria against which each vehicle is evaluated.

2 Methodology

A three-part computational routine was developed to evaluate the Baja vehicle's dynamic response. The code's first section inputs data from the vehicle's geometry, suspension system, and model matrices (mass, stiffness, and damping). The following section generates the road surface roughness profiles from power spectral density functions and converts them into time-domain signals. Finally, the third section performs the numerical integration of the equations of motion using Newmark's method. Each section is validated using commercial software or data from the literature. The outputs are the displacement, velocity, and acceleration signals for each degree of freedom

of the vehicle model. Concepts and equations needed for developing each part of the code are described in detail in the following subsections.

2.1 Road profile model

The stochastic pavement surface roughness is modeled using Power Spectral Density (PSD) functions, according to ISO 8608:1995 [4], which establishes a methodology to generate road surface profiles in the frequency domain for different road qualities. According to Sekulić et al. [5], the PSD from this standard can be converted to temporal frequency (f) using the equation below

$$G_d(f) = v^{w-1} G_d(n_0) \left(\frac{n_0}{f}\right)^w, \tag{1}$$

where v is the vehicle's speed, $G_d(n_0)$ is the roughness coefficient at a reference spatial frequency n_0, and w is the PSD exponent. According to the standard, the PSD exponent is 2 for constant speed, and the reference frequency is $n_0 = 0,1$ cycles/m. The roughness coefficients are defined for eight classes of roads with different qualities and can be found in ISO 8608:1995 [4]. In this research, a class H road was considered to simulate the rough terrain conditions in which SAE tests are performed.

Since the vehicle is three-dimensional, it is necessary to establish another roughness profile for the left wheels. It can be done by assuming that the road surface is isotropic, and using a coherence function to relate left and right track profiles [4], as shown in Eq. 2.

$$G_{dc}(f) = \gamma(f) G_d(f) \tag{2}$$

$G_{dc}(f)$ is the road surface profile cross-PSD imposed on the front left wheel, and $\gamma(f)$ is the coherence function that relates it to the right PSD [5]. The coherence function is given by Eq. 3, where v_l is a cut-off frequency of 0,2 cycles/m, determined experimentally, and depends on the frequency (f) and the vehicle's speed (v).

$$\gamma(f) = \frac{v_l^2}{v_l^2 + \left(\frac{f}{v}\right)^2} \tag{3}$$

From the PSD functions, a signal in the time domain can be created to represent the tracks' vertical profile as a time function using equations proposed by Sekulić et al. [5]. Therefore, the vertical displacements imposed on the front right wheel are calculated from Eq. 4

$$z(t) = \sum_{k=1}^{N} \sqrt{2 G_d(f_k) \Delta f} \cos\left(2\pi f_k t + \psi_k\right), \tag{4}$$

where N is the number of intervals in the frequency domain, $G_d(f_k)$ is the PSD of the right front wheel, Δf is the frequency resolution, and ψ_k is an independent random phase angle uniformly distributed between 0 and 2π.

The time signal for the front left wheel is generated through Eq. 5, which considers the same parameters as for the front right wheel, and also the cross-PSD for the left side ($G_{dc}(f_k)$), and another random variable (ϕ_k) with a uniform distribution between 0 and 2π.

$$z_{dc}(t) = \sum_{k=1}^{N} \left[\sqrt{2 G_d(f_k) \Delta f} \cos\left(2\pi f_k t + \psi_k\right) + \sqrt{2 \left(G_d(f_k) - G_{dc}(f_k)\right) \Delta f} \cos\left(2\pi f_k t + \phi_k\right) \right] \tag{5}$$

Velocity and acceleration vectors can be obtained by differentiating $z_d(t)$ and $z_{dc}(t)$ with respect to time (t). The rear wheels are subjected to the same roughness profile as the front ones with a specific delay since they are

aligned. This delay (T) is determined by the ratio between the wheelbase (l) and the vehicle's speed (v). Hence, to create the displacements applied to the rear wheels, a Heaviside function can be applied to the front profiles (Eq. 6) [6].

$$f_t(t) = f(t-T)u(t-T) \tag{6}$$

2.2 Dynamic analysis

The dynamic system investigated in this paper can be represented by eight equations of motion described in matrix form, according to Eq. 7. $\mathbf{M}$, $\mathbf{C}$, and $\mathbf{K}$ are the vehicle's mass, damping, and stiffness matrices, $\overrightarrow{\ddot{z}}(t)$, $\overrightarrow{\dot{z}}(t)$, and $\overrightarrow{z}(t)$ are acceleration, velocity, and displacement vectors, and $\overrightarrow{F}(t)$ is the vector of external forces.

$$\mathbf{M}\overrightarrow{\ddot{z}}(t) + \mathbf{C}\overrightarrow{\dot{z}}(t) + \mathbf{K}\overrightarrow{z}(t) = \overrightarrow{F}(t) \tag{7}$$

A full-car model was adopted to simulate the dynamic behavior of a Baja-type vehicle. It represents a three-dimensional car with eight degrees of freedom (DoF), consisting of four non-sprung masses representing the wheels and two sprung masses, one for the car body and the other for the driver's seat. These elements are connected by linear springs and dampers, which simulate the vehicle's suspension system and tires [7, 8]. The matrices and vectors adopted to represent the full-car model can be found in Fossati et al. [7]; they will not be described here due to space limitations. Newmark's direct integration method is adopted to solve these equations [9]. Figure 1 shows a schematic drawing of the model.

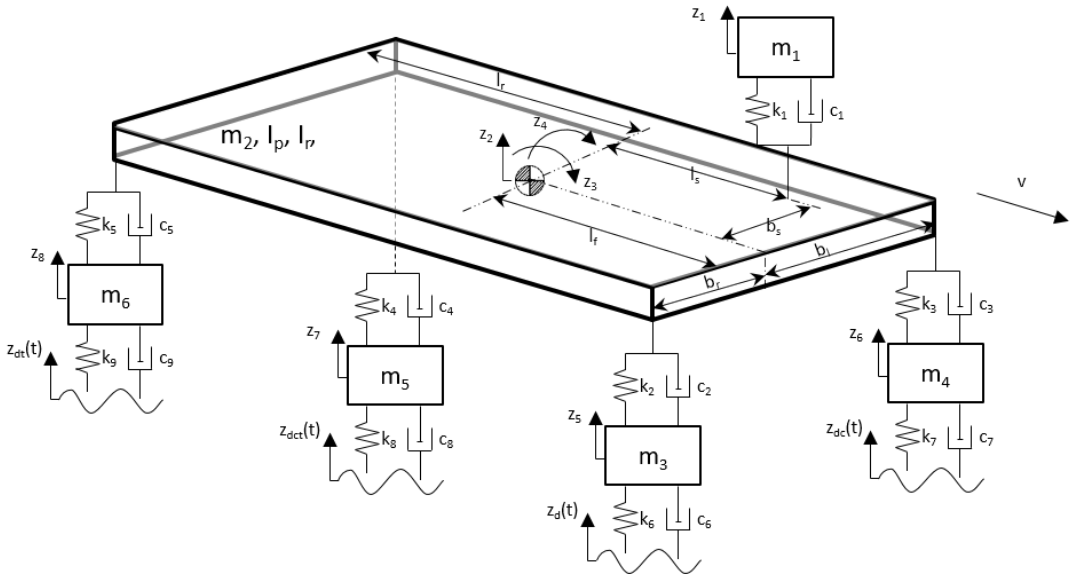

Figure 1. Full-car vehicle model.

The conductor's seat mass is represented by m_1, which has stiffness and damping coefficients k_1 and c_1. The car body is represented by m_2, in addition to pitch and roll moments I_p and I_r. Masses m_3 and m_4 simulate front right and left wheels, respectively, and masses m_5 and m_6 represent the rear wheels. These unsprung masses are connected to the car body by the springs and dampers k_2, c_2, k_3, c_3, k_4, c_4, k_5, and c_5, representing the suspension system. The stiffness and damping coefficients of the tires are given by k_6, c_6, k_7, c_7, k_8, c_8, k_9, and c_9. The excitations imposed by the track on the right and left front wheels are given by $z_d(t)$ and $z_{dc}(t)$, respectively, and $z_{dt}(t)$and $z_{dct}(t)$ for the right and left rear wheels. The eight DoF are described in Table 1.

Table 1. Full-car model degrees of freedom.

DoF	Description	DoF	Description
z_1	Driver's seat vertical displacement (m)	z_5	Front right wheel vertical displacement (m)
z_2	Car body vertical displacement (m)	z_6	Front left wheel vertical displacement (m)
z_3	Car body pitch angle (rad)	z_7	Rear left wheel vertical displacement (m)
z_4	Car body roll angle (rad)	z_8	Rear right wheel vertical displacement(m)

Some parameters needed to perform the dynamic analysis were obtained through physical tests, and others were obtained from data from the literature. The masses of the car body and wheels were obtained experimentally, as well as the suspension and tire stiffness. Damping coefficients and moments of inertia were obtained from the literature. Table 2 shows the values of each parameter used in the simulation.

Table 2. Values of mechanical and geometric parameters for the full-car model.

Variable	Value	Variable	Value	Variable	Value
k_1	15000 N/m	c_2, c_3, c_4, c_5	1520,73 N.s/m	I_r	41.6 kg.m^2
k_2, k_3	14420 N/m	m_1	82.4 kg	l_s	-0.0159 m
k_4, k_5	23560 N/m	m_2	191.7 kg	l_f	0.8367 m
k_6, k_7	39372 N/m	m_3, m_4	9.72 kg	l_r	0.5666 m
k_8, k_9	47820 N/m	m_5, m_6	9.16 kg	b_s	-0.019 m
c_1, c_6, c_7, c_8, c_9	150 N.s/m	I_p	56.4 kg.m^2	b_l, b_r	0.66 m

3 Results and discussion

3.1 Validation

Each code section was validated through comparatives with commercial software or data from the literature to ensure the correct implementation of the calculations. The pavement roughness temporal signal generator was verified by converting the signal back into the frequency domain using the Matlab function "periodogram.m" and comparing it with the original PSD, as illustrated in Figure 2.

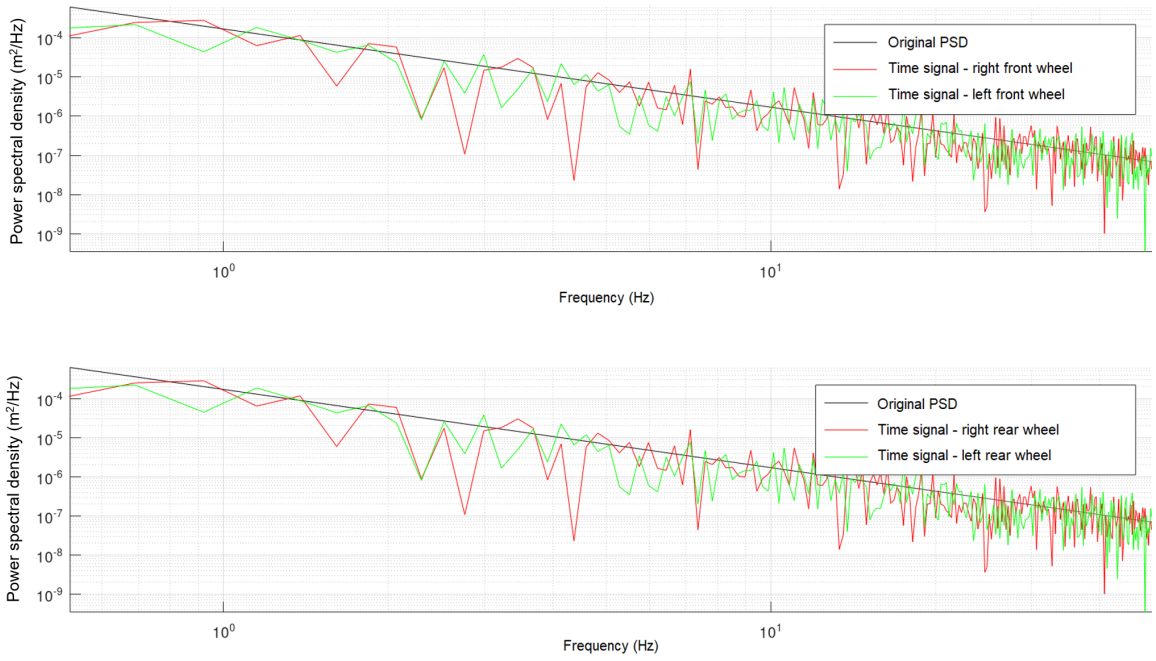

Figure 2. Comparison between the frequency spectra from original PSD and from time signals.

The geometry, mass, and stiffness values used in Meng et al. [8] were replicated in the implemented code to validate the full-car model, and a modal analysis was performed. The results of natural frequency and vibration modes were compared, and the equality was verified.

Finally, the numerical integration routine was certified through the solution of a simple dynamic system consisting of four degrees of freedom. Numerical and analytical results were compared, evidencing the accuracy of the code, as shown in Table 3.

Table 3. Displacement results at $t = 5$ s obtained analitically and through Newmark's integration method.

DoF	Analytical solution	Numerical solution	Difference (%)
1	-0.5160	-0.5160	0.0063
2	-0.0438	-0.0438	0.0190
3	-0.7969	-0.7968	0.0080
4	0.4335	0.4334	0.0159

3.2 Baja-type vehicle dynamic analysis

Tables 4 and 5 show the vehicle's natural frequencies and vibration modes, respectively. Those values were obtained during the modal analysis step of the code and are related to mass and stiffness matrices.

Table 4. Natural frequencies of Baja-type vehicle, in Hz.

f_1	f_2	f_3	f_4	f_5	f_6	f_7	f_8
1.7452	3.2094	3.3004	3.6689	11.9282	11.9953	14.2103	14.2121

Table 5. Vibration modes of Baja-type vehicle.

DoF	$\vec{C}_1$	$\vec{C}_2$	$\vec{C}_3$	$\vec{C}_4$	$\vec{C}_5$	$\vec{C}_6$	$\vec{C}_7$	$\vec{C}_8$
z_1	0.9291	-0.5170	0.0928	0.0165	0.0000	-0.0007	0.0006	0.0000
z_2	0.3151	0.6445	-0.1123	-0.0141	-0.0000	0.0209	-0.0230	-0.0006
z_3	0.0041	-0.3441	-0.9022	-0.0025	-0.0000	-0.0582	-0.0462	-0.0012
z_4	0.0098	-0.0611	0.0143	-0.9180	-0.0596	0.0001	0.0020	-0.0753
z_5	0.0872	0.2581	0.1895	-0.1832	0.7039	-0.7060	-0.0103	0.0300
z_6	0.0836	0.2814	0.1840	0.1761	-0.7047	-0.7052	-0.0087	-0.0304
z_7	0.1043	0.1706	-0.2211	0.2091	0.0465	-0.0147	0.7249	-0.6852
z_8	0.1086	0.1425	-0.2145	-0.2201	-0.0466	-0.0146	0.6868	0.7232

Some characteristics of each vibration mode can be inferred from the previous table. The first two vibration modes are associated with natural frequencies of 1.7452 Hz and 3.2094 Hz, respectively, and mainly excite the driver's seat. In the second mode, there is also significant excitation of the vertical displacement of the car body. The third and fourth vibration modes induce excitations in the car body's pitch and roll degrees of freedom, with natural frequencies of 3.3004 Hz and 3.6689 Hz. The first four modes, corresponding to the suspended masses that form the vehicle model, are related to low frequencies, ranging between 1.7452 Hz and 3.6698 Hz.

The following modes are associated with unsprung masses, i.e., the vehicle's wheels, and have higher natural frequencies. The fifth and sixth modes have natural frequencies of 11.9282 Hz and 11.9953 Hz, respectively, and excite the degrees of freedom relative to the right and left wheels of the front axle. The seventh and eighth modes excite the rear axle wheels, predominating the excitation of the left wheel in the seventh mode, with a natural frequency of 14.2013 Hz. In the eighth mode, the excitation of the right rear wheel predominates, with a natural frequency of 14.2121 Hz.

According to Chaffin et al. [10], the frequency range from 0 to 2 Hz commonly manifests discomfort in human beings due to interference in the vestibular system; the range from 2 to 30 Hz imposes resonances on the body, and frequencies above 20 Hz affect muscles, tendons, and skin. Results indicate that the first vibration modes of the seat can lead to discomfort, and the other modes can harm the driver. Hence, the comparison with the exposure to

vibration levels to which the driver is subject must be verified with the stipulated criteria by the ISO 2631:1997 [2] standard.

The vertical displacement response of the driver's seat, vehicle body, and left front wheel are shown in Figure 3. The magnitudes of the vertical displacements for these three degrees of freedom are similar. However, it is possible to notice the damping effect when comparing the displacements suffered by the wheel and the driver. The effect of the suspension system is evident in the smoothing of the driver's seat displacement curve concerning the wheel curve.

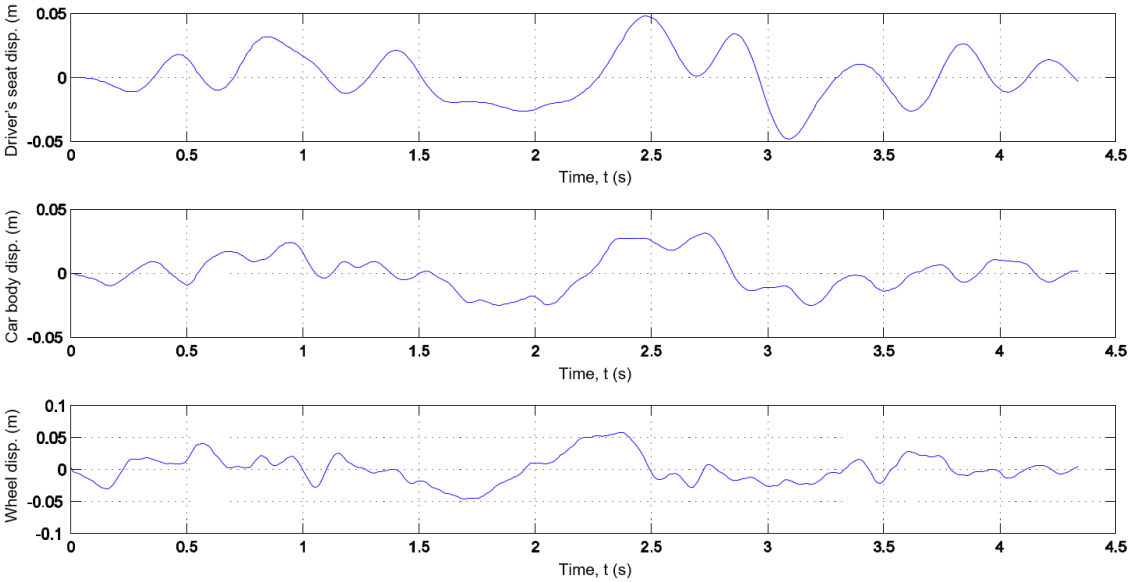

Figure 3. Vertical displacements of driver's seat, car body and left front wheel over the simulation time interval.

The vertical acceleration results for the degrees of freedom mentioned above are shown in Figure 4. Once again, the damping effect of the suspension system is evident when comparing the levels of acceleration suffered by the front left wheel with those reaching the driver. There is a tenfold reduction in amplitude and curve smoothing.

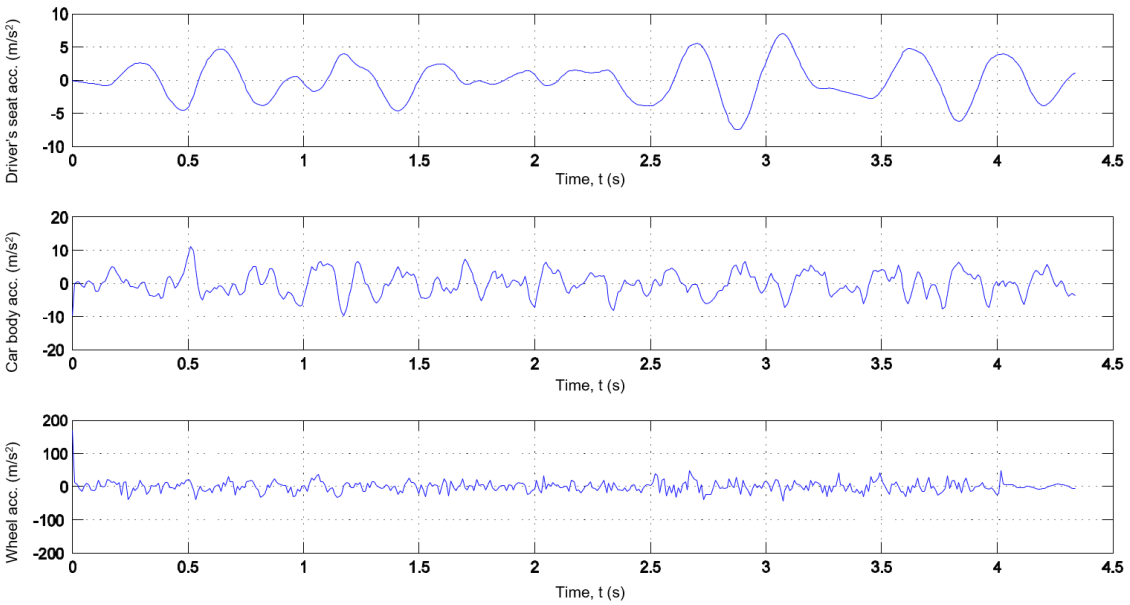

Figure 4. Vertical acceleration of driver's seat, car body and left front wheel over the simulation time interval.

4 Conclusions

This work presented the dynamic analysis of a Baja-type vehicle traveling over rough terrain. The accuracy of the computational routine developed was proved by validating each section of the code with commercial software or data from the literature. The similarity between outputs from the code and the gathered data demonstrates the correct construction of the computational routine and the results' reliability. Also, the program can easily be adapted to analyze other vehicles and road conditions.

The effect of the suspension system was noted in the damping of the driver's displacement and acceleration signals. A decrease in vibration amplitude is seen when signals are compared to wheel degree of freedom signals, primarily in terms of acceleration. In addition, curve smoothing is also perceived.

Future research may deepen the knowledge of the suspension system effect by varying parameters of stiffness and damping. It is also possible to carry out a comfort analysis according to the ISO 2631 standard to guarantee accelerations within acceptable limits in longer events, such as the endurance test, which is a 4 hours race in off-road terrain.

References

[1] O. T. Perseguim. *Dinâmica veicular relativa ao ride de veículos e métricas para sua avaliação*. PhD thesis, Universidade de São Paulo, São Carlos, 2005.

[2] ISO 2631:1997. Mechanical Vibration and Shock – Evaluation of human exposure to whole-body vibration. Standard, International Organization for Standardization, Geneva, CH, 1995.

[3] SAE BRASIL, 2021.

[4] ISO 8608:1995. Mechanical Vibration –Road Surface Profiles – Reporting of Measured Data. Standard, International Organization for Standardization, Geneva, CH, 1995.

[5] D. Sekulić, V. Dedović, S. Rusov, S. Šalinić, and A. Obradović. Analysis of vibration effects on the comfort of intercity bus users by oscillatory model with ten degrees of freedom. *Applied Mathematical Modelling*, vol. 37, n. 18-19, pp. 8629–8644, 2013.

[6] G. P. d. Santos. Simulação da interação veículo-estrutura-pavimento em pontes rodoviárias. mathesis, Universidade Federal do Rio Grande do Sul, Porto Alegre, 2020.

[7] G. G. Fossati, L. F. F. Miguel, and W. J. P. Casas. Multi-objective optimization of the suspension system parameters of a full vehicle model. *Optimization and Engineering*, vol. 20, n. 1, pp. 151–177, 2018.

[8] R. Meng, N. Xie, and L. Wang. Multiobjective game method based on self-adaptive space division of design variables and its application to vehicle suspension. *Mathematical Problems in Engineering*, vol. 2014, pp. 1–13, 2014.

[9] S. S. Rao. *Mechanical Vibrations*. Prentice Hall, New Jersey, 5 edition, 2004.

[10] D. B. Chaffin, G. B. J. Andersson, and B. J. Martin. *Occupational Biomechanics*. Wiley-Interscience, 4 edition, 1999.

Authorship statement. The authors hereby confirm that they are the sole liable persons responsible for the authorship of this work, and that all material that has been herein included as part of the present paper is either the property (and authorship) of the authors, or has the permission of the owners to be included here.